Nanocontainers Formed by Self-Assembly of Poly(ethylene oxide)-*b*-poly(glycerol monomethacrylate)−Drug Conjugates

Cristiano Giacomelli, Vanessa Schmidt, and Redouane Borsali*,†

Laboratoire de Chimie des Polymères Organiques (LCPO), ENSCPB, Université Bordeaux 1, 16 Av. Pey Berland, 33607 Pessac Cedex, France

Received November 6, 2006; Revised Manuscript Received January 9, 2007

ABSTRACT: The synthesis, self-assembly behavior, and delivery properties of poly(ethylene oxide)-*b*-poly(glycerol monomethacrylate)− (PEO-*b*-PG2MA−) drug conjugates is herein described. Double hydrophilic PEO-*b*-PG2MA copolymers synthesized by atom transfer radical polymerization (ATRP), using a PEO-based macroinitiator, were used for post-polymerization conjugation to the hydrophobic nonsteroidal anti-inflammatory agent indomethacin (IND). IND contents ranging from 15 to 49% w/w_p were attached to the same polymer precursor via Steglich esterification, leading to amphiphilic block copolymer−drug conjugates (PEO-*b*-(PG2MA-IND)). Dynamic light scattering (DLS) and transmission electron microscopy (TEM) experiments revealed that PEO-*b*-(PG2MA-IND) copolymer chains self-assemble into spherical nanoparticles in water, whose hydrodynamic size ($2R_H$ = 24−100 nm) and morphology (micelles or vesicles) are dictated by both the amount of IND and the PG2MA block length. Interestingly, such a particular system was also proven to be able to stabilize, transport and deliver physically encapsulated (free) IND (F-IND). The maximum F-IND loadings ranged from 13 to 20% w/w_p, thus reaching remarkable IND payloads (i.e., covalently bound B-IND + physically entrapped F-IND) as high as 58% w/w_p. However, self-organization for F-IND loaded samples with more than 50% w/w_p IND originated vesicular morphologies instead of micelles and provoked a huge increase in the size of the objects. The release of IND is a pH-dependent process, which is governed by intrinsic molecular characteristics of F-IND (aqueous dissociation behavior) and pH-sensitivity of ester linkages in the conjugates. At approximately neutral pH, the ester bound linkages are stable and the diffusion of F-IND out of the carrier is favored, whereas sustained release with slow kinetics takes place under acidic pH conditions.

Introduction

Recent advances in controlled/living polymerization processes have encouraged the preparation of a multitude of macromolecules with controllable architecture, functionality, composition and topology.[1] Often combining chemically distinct monomers and successive polymerization techniques, well-defined polymers exhibiting nanophase separation have been synthesized. Such materials can originate—after equilibrium and rather complex preparation procedures—thermodynamically stable nano-objects in solution (micelles, vesicles, etc.),[2−4] which have been increasingly and successfully tested as nanosized containers in many fields, and particularly in drug delivery. The use of these assemblies as delivery vehicles is motivated principally by their ability to incorporate and release poorly water-soluble, hydrophobic and/or highly toxic compounds, also minimizing drug degradation and wastage, and hence increasing bioavailability.[5−9] In addition, specific drug targeting through micellar drug delivery vehicles has been achieved either by functionalizing the micelle surface[9−14] or by designing smart functions as physical or chemical stimuli-sensitivity.[15]

In this regard, poly(ethylene oxide) (PEO) and poly(2-(methacryloyloxy)ethyl phosphorylcholine) (PMPC) have been preferred as corona-forming blocks of assemblies used in biomedical applications due to their clinically proven exceptional biocompatibility, in spite of the large variety of synthetic polymers easily accessible.[5,16] Conversely, given that the inner core is presumably surrounded by a biocompatible shell, the selection of ore-forming blocks comprises much wider variety of polymers, thus allowing fine-tuning of micelle properties in order to optimize drug delivery parameters such as loading content (payload capacity), loading efficiency, partition coefficient between aqueous environment and micelle core and release kinetics. Indeed, the chemical nature of both core-forming block and loaded drug has utmost implications in the above-mentioned delivery related parameters. Ideally, to achieve very high loading into micelles, the solubility parameters of the solubilizate (drug) and the core-forming polymer block should be the same (i.e., the Flory−Huggins interaction parameter (χ) should be zero). As suggested by Eisenberg et al.,[5,6] in fact there is no universal core-forming block, because each probe or drug is unique. Therefore, it is important to match the probe or drug with the core-forming polymer in order to achieve maximal loading into the micelles. Last but not least, the block copolymer composition and molecular weight as well as the architecture (flexibility, rigidity, linear, cyclic, stars, etc.) affect remarkably the performance of delivery systems.

Among other potent drugs showing non-negligible side effects following administration of conventional non-formulated products, indomethacin (IND), 1-(4-chlorobenzoyl)-5-methoxy-2-methyl-1*H*-indole-3-acetic acid, a potent nonsteroidal anti-inflammatory drug (NSAID),[17] causes important irritation of gastrointentinal mucosa and toxicity to central nervous system as a consequence of high plasma levels. NSAIDs such as IND are good drug models for studying micelle formation. Leroux et al.[18] reported that 6−14% w/w_p (weight of drug/weight of polymer × 100) IND can be encapsulated in micelles made from PEO and poly(*t*-butyl methacrylate) (P*t*BuMA), poly(ethyl acrylate) (PEA) or poly(*n*-butyl acrylate) (P*n*BuA) diblock copolymers. Similarly, using poly(lactic acid) (PLA) as the core-forming block, Choi and Kim[19] achieved IND loadings of 8−9%

* Corresponding author. E-mail: borsali@enscpb.fr.
† Present address: CERMAV-CNRS, BP53, 38041, Grenoble Cedex 9, France. E-mail: borsali@cermav.cnrs.fr.

10.1021/ma062562u CCC: $37.00
Published on Web 02/21/2007

w/w_p in PEO-*b*-PLA micelles. The use of polycaprolactone (PCL) or poly(β-benzyl-L-aspartate) (PBLA) as the hydrophobic block revealed slightly higher IND payload capacities for PEO-*b*-PCL (17−42% w/w_p) and PEO-*b*-PBLA (ca. 20% w/w_p) micelles, as reported by Lee et al.[20,21] and Kataoka et al.,[22] respectively. In all these systems, IND molecules were physically entrapped inside the micelle core.

In different approaches, nanoparticles with improved IND payload were designed by Bertin et al.,[23] who synthesized block copolymers via ring-opening metathesis polymerization (ROMP) with sequential monomer addition of α-norbornenyl indomethacin and α-norbornenyl hexa(ethylene glycol) monomers. The resulting amphiphilic block copolymer−drug conjugates contained a remarkably high density of covalently linked IND (30−60% w/w_p), however their self-assembly originated quite large particles (130−1600 nm). Similarly, colloidal particles (>250 nm) carrying IND (5−70% w/w_p) covalently linked to their core were prepared via dispersion ROMP by Quémener et al.[24]

Within this context, we have contemplated the design of micellar nanocontainers that could show optimized performance for IND delivery (i.e., high payload and controlled release). The herein reported approach is based on the synthesis of double hydrophilic poly(ethylene oxide)-*b*-poly(glycerol monomethacrylate) (PEO-*b*-PG2MA) block copolymer, which exhibits pendent hydroxyl groups in the PG2MA block, followed by its post-polymerization conjugation to IND via Steglich esterification. The resulting amphiphilic macromolecule−drug conjugates (PEO-*b*-(PG2MA-IND)) were found to self-assemble into spherical micellar nanoparticles or vesicles in selective solvent (water), therefore originating a particular core−shell system in which the core-forming block (PG2MA-IND) resembled the drug to be physically encapsulated (IND). Hence, such micellar nanocontainers are able to transport two or more hydrophobic molecules−IND chemically linked to the polymer via acid-sensitive bounds and another physically entrapped−which can be released either simultaneously in a pH-triggered process or selectively by initial passive diffusion of unbound species.

Experimental Section

Materials. α-Methoxy-ω-hydroxy poly(ethylene oxide) (CH_3O-PEO_x-OH, Fluka, M_n = 5000 g/mol, M_w/M_n = 1.02), α-bromoisobutyryl bromide (Aldrich, 98%), *N*,*N*′-dicyclohexylcarbodiimide (DCC, Fluka, 98%), 4-dimethylaminopyridine (DMAP, Aldrich, 98%),and indomethacin (IND, Fluka, 99%) were used as received. Glycerol monomethacrylate (G2MA) was kindly donated by Röhm Methacrylates.

Synthesis of PEO Macroinitiators. Bromo-terminated PEO macroinitiators were prepared by reacting hydroxyl end groups with α-bromoisobutyryl bromide as reported in the literature[25] and described in the Supporting Information (SI). Pure white products were obtained after three times precipitation in cold diethyl ether.

Atom Transfer Racial Polymerization (ATRP). In a typical procedure, G2MA monomer (5.75 g, 36 mmol) and methanol as solvent (15.0 mL) were charged to a dry 100 mL Schlenk flask. After being purged with nitrogen during 30 min to remove dissolved oxygen, the solution was cannulated under nitrogen into another Schlenk tube, previously evacuated and filled with nitrogen, containing Cu^IBr (0.13 g, 0.90 mmol), $MeO-PEO_{113}-Br$ macroinitiator (4.49 g, 0.90 mmol), 2,2′-bipyridyl (bpy) ligand (0.28 g, 1.80 mmol), and a magnetic stirrer. The reaction mixture became immediately dark brown and progressively more viscous, indicating the onset of polymerization. After 3 h at 20 °C, ^{1}H NMR analysis indicated that more than 94% G2MA had been polymerized. The reaction was then stopped by opening the flask to air and adding 40 mL of aerated methanol. The mixture was subsequently passed through a silica gel column in order to remove the spent ATRP catalyst. The final white product was obtained by precipitation in diethyl ether, and it was vacuum-dried overnight.

Indomethacin Conjugation. Conjugation of indomethacin (IND) to pendent hydroxyl groups of PG2MA segments was achieved using Steglich esterification. In a typical procedure, CH_3O-PEO_{113}-*b*-$PG2MA_{40}$ diblock (0.40 g, 0.032 mmol, 2.56 mmol OH groups) and IND (0.46 g, 1.28 mmol) were dissolved in 5.0 mL of dry DMF. Subsequently, DCC (0.26 g, 1.28 mmol) and DMAP (catalytic 10 mol % amount) dissolved in DMF (1.0 mL) were added dropwise. The mixture was left to react at room temperature during 72 h. Afterward, DMF was almost completely removed under reduced pressure. Then, 10.0 mL of THF were added to redissolved polymer−drug conjugate. The remaining solid byproducts (urea) were filtered off, and the solvent volume was reduced to 4−5 mL. Finally, the copolymer−drug conjugate was obtained after precipitation in a 10-fold excess of cold diethyl ether, conditions under which free IND is soluble, thus allowing the removal of unreacted drug. The IND amount effectively attached to the polymer was determined by ^{1}H NMR and UV−vis spectroscopy.

Polymer Characterization. (a) ^{1}H Nuclear Magnetic Resonance (^{1}H NMR). 400 MHz ^{1}H NMR spectra were acquired using an Avance DPX 400 spectrometer. For PEO-*b*-PG2MA diblock copolymers, D_2O or MeOD was used as solvent, while DMF-d_7 was chosen for PEO-*b*-(PG2MA-IND) polymer−drug conjugates.

(b) Gel Permeation Chromatography (GPC). Number-average molar mass (M_n) and molar mass distribution (M_w/M_n) values were determined by GPC in DMF containing 1.0 g/L LiBr at a flow rate of 1.0 mL/min using a PLgel 5 μm guard column and a series of two PLgel 5 mm Mixed-C columns and Jasco 1530 RI (set at 40 °C) and 875 UV detectors. Calibration was performed using a series of near-monodisperse polystyrene (PS) standards.

General Procedures for Sample Preparation. (a) Aqueous Micellar Solutions. Dilute PEO_x-*b*-($PG2MA_y$-IND_z) (here and throughout the text, subscripts *x* and *y* refer to the mean degree of polymerization (DP) of each block, whereas *z* stands for the number of IND molecules attached to the PG2MA segment) aqueous solutions (C_p = 1.0 mg/mL) were prepared using the volatile organic solvent approach. Typically, 7.0 mg of polymer−drug conjugate were dissolved in 0.3 mL of distilled THF (good solvent for both blocks) in a closed vial. The solution was allowed to stir for at least 3 h. Micellization was subsequently induced by slow addition (0.33 mL/min) of 7.0 mL of Milli-Q water. The solution was then stirred overnight and purged gently with N_2 during ca. 12 h to speed up THF evaporation. ^{1}H NMR spectra of micellar solutions recorded before (control) and after such a procedure revealed the complete disappearance of chemical shifts associated with protons in the THF structure.

(b) Drug-Loaded Micelles. Drug-loaded micelles were prepared using essentially the same procedure as described above, except that in this case 50% w/w_p (1.75 mg) IND was dissolved along with the polymer−drug conjugate (3.50 mg) in THF (0.15 mL). After micellization (induced by the slow (0.33 mL/min) addition of 3.5 mL of Milli-Q water) and elimination/evaporation of remaining THF, unloaded IND that precipitated out of the solution as a white solid was removed during the micelle filtration process using o.d. = 0.45 μm pore size nylon filters.[26] Finally, the drug content encapsulated inside the micelle was determined by the UV−vis spectrometry as described below.

(c) Determination of Drug Loading Content in the Micelles. The drug content encapsulated inside the micellar carrier was determined by the UV−vis spectrometry using the standard addition method. For these experiments, 50 μL aliquots of each micellar solution were diluted in approximately 3.0 mL of THF, thus provoking demicellization of polymer chains. Afterward, the UV−vis absorption intensity at 320 nm (λ_{max}) was measured as a function of known added aliquots (0, 15, 30, 45, and 60 μL) of 1.6 mg/mL (4.5 mmol/L) IND. Linear fitting of experimental data generated straight lines, from which the "negative volume" of added IND corresponding to zero UV−vis absorption was obtained, and accordingly the amount of IND present in the original micellar

solution was calculated.[26] The loading efficiency and the drug content were calculated using the eqs 1 and 2, respectively.

$$\text{loading efficiency (LE) (\%)} = \frac{\text{mass of probe in micelles (g)}}{\text{mass of probe used (g)}} \times 100 \quad (1)$$

$$\text{drug content (\% w/w}_p\text{)} = \frac{\text{mass of drug in micelles (g)}}{\text{mass of micelles (g)}} \times 100 \quad (2)$$

(d) In Vitro Release Kinetics. Release experiments were conducted using the dialysis method. In a typical experiment, 7.0 mL of nanoparticles solutions was sealed in a dialysis bag (Spectrum, MWCO = 25 000 g/mol, shown in Figure S1), which was immersed in 2.0 L of 0.025 mol/L phosphate buffer solution at pH either 2.1 or 7.4. This buffer solution was periodically changed to ensure release kinetics under nearly sink conditions. In order to follow the release kinetics, aliquots (50 μL) were withdrawn regularly from the micellar solution, and diluted into 3.0 mL of THF, thus causing disassembly of block copolymer−drug conjugates into molecularly dissolved chains. The released drug content was determined directly by UV−vis spectrometry using typical indomethacin absorbance maximum at $\lambda_{max} = 320$ nm, as described above.

Dynamic Light Scattering (DLS). DLS measurements were performed using an ALV laser goniometer, which consists of a 22 mW HeNe linear polarized laser operating at a wavelength of 632.8 nm and an ALV-5000/EPP multiple τ digital correlator with 125 ns initial sampling time. The copolymer solutions were maintained at a constant temperature of 25.0 ± 0.1 °C in all experiments. The accessible scattering angles range from 15 to 150°. The solutions were placed in 10 mm diameter glass cells. The minimum sample volume required for DLS experiments was 1 mL. Data were collected using ALV Correlator Control software and the counting time varied for each sample from 300 to 900 s. The relaxation time distributions, $A(t)$, were in the sequence obtained using CONTIN analysis[27] of the autocorrelation function, $C(q,t)$. The relaxation frequency, Γ ($\Gamma = \tau^{-1}$) depends generally on the scattering angle, and in the case of a diffusive particle, this frequency is q^2-dependent.[28] Consequently, the apparent diffusion coefficient (D_{app}) at a given copolymer concentration (C_p) is calculated from

$$\frac{\Gamma}{q^2}\Big|_{q\to 0} = D_{app} \quad (3)$$

where q is the wavevector defined as

$$q = \frac{4\pi n}{\lambda}\sin\left(\frac{\theta}{2}\right) \quad (4)$$

and λ is the wavelength of the incident laser beam (632.8 nm) and θ is the scattering angle. The hydrodynamic radius (R_H) (or diameter, $2R_H$) is calculated from the Stokes−Einstein relation

$$R_H = \frac{k_B T}{6\pi\eta\Gamma} q^2 = \frac{k_B T}{6\pi\eta D_{app}} \quad (5)$$

where k_B is the Boltzmann constant, T is the temperature of the sample, and η is the viscosity of the medium.

Transmission Electron Microscopy (TEM). TEM images were recorded using a CM 120 Philips microscope operating at 120 kV, and equipped with a USC1000-SSCCD 2k × 2k Gatan camera. To prepare the TEM samples, 5 μL of an aqueous solution of block copolymer micelles was dropped onto a carbon-coated copper grid, which was rendered hydrophilic by UV/ozone treatment. Excess micelle solution was gently removed using absorbent paper. Samples were then negatively stained by adding a 5 μL droplet of 2% sodium phosphotungstate solution at pH 7.5, and the excess solution was again removed prior to drying under ambient conditions.

UV—Vis Spectroscopy. UV−vis spectra were recorded using a Varian Cary 300 UV−vis spectrophotometer. For the measurements, 3.0 mL of solution were placed in a 10 mm square quartz cell. All spectra were recorded after baseline correction for solvent from air-equilibrated solutions in the 300−450 nm wavelength range at scan rate of 600 nm/min (0.1 s integration per 1.0 nm).

Results and Discussion

Synthesis of Diblock Copolymers and Conjugates. Double hydrophilic diblock copolymer−drug conjugates showing self-assembly properties have been prepared as illustrated in Figure 1a. First, poly(ethylene oxide)-*b*-poly(glycerol monomethacrylate) (PEO-*b*-PG2MA) block copolymers were synthesized by ATRP of G2MA in methanol using PEO macroinitiators and Cu/bpy catalyst, as previously described elsewhere by Armes et al.[29] Block copolymers systems with narrow molecular weight distributions ($M_w/M_n < 1.20$) were obtained, as shown in Table 1 and in Figure S2.

In the following step, the pendent hydroxyl groups of PG2MA blocks were used for post-polymerization conjugation to the hydrophobic drug IND by Steglich esterification (Figure 1a), which is a mild reaction allowing the conversion of sterically demanding systems. In contrast to the quite simple organic chemistry implied in esterification reactions between hydroxylated and carboxylated small molecules, analogous polymers frequently require forcing conditions to achieve the desired degree of modification.[30] Table 2 shows the molecular characteristics as assessed by ^{1}H NMR and UV−vis (Supporting Information, section 3) of amphiphilic block copolymer−drug conjugates synthesized and hereinafter investigated. Satisfactory agreement between results collected using NMR or UV was observed, and UV analysis was chosen to discuss the data due to its good analytical reliability. The coupling was also confirmed in all cases by GPC−UV analysis (data not shown).

As can be observed in Table 2, the conversions typically remained in the range of 24 − 72%, whereas a slight decrease apparently occurred upon the increase in the molecular weight of PG2MA block. The incomplete reaction is most probably explained by the sterical hindrance imposed by first grafted IND bulky molecules and the difference in the reactivity of primary and secondary hydroxyl groups in the PG2MA structure.[30,31] These results are in good agreement with other reports on the esterification of hydroxyl substituted macromolecules.[31,32]

The final drug content clearly depended, however, on the targeted IND/OH molar ratio. As a result, distinct drug amounts were covalently attached to the same polymer precursor, yielding block copolymer−drug conjugates in which the volume fraction of G2MA-IND ($\phi_{G2MA-IND}$) varied from 0.22 to 0.68. Besides, samples exhibiting fairly similar $\phi_{G2MA-IND}$ values but different PG2MA block lengths were synthesized. It is also meaningful to note the weight percentage (wt %) of IND in the polymer−indomethacin conjugates, which varied between 15 and 49%. These values are fairly comparable to those reported by Bertin et al.[23] and Quémener et al.,[24] who polymerized norbornenyl-modified indomethacin monomers.

The self-assembly of block copolymers has been the subject of comprehensive theoretical and experimental studies,[33] and it is nowadays well-established that the volume fraction (ϕ) of each constituting segments is a major driving force—along with the overall degree of polymerization (DP) and Flory−Huggins interaction parameter (χ)—that defines the thermodynamic-stable morphology. Roughly, spherical core−shell micelles are favored

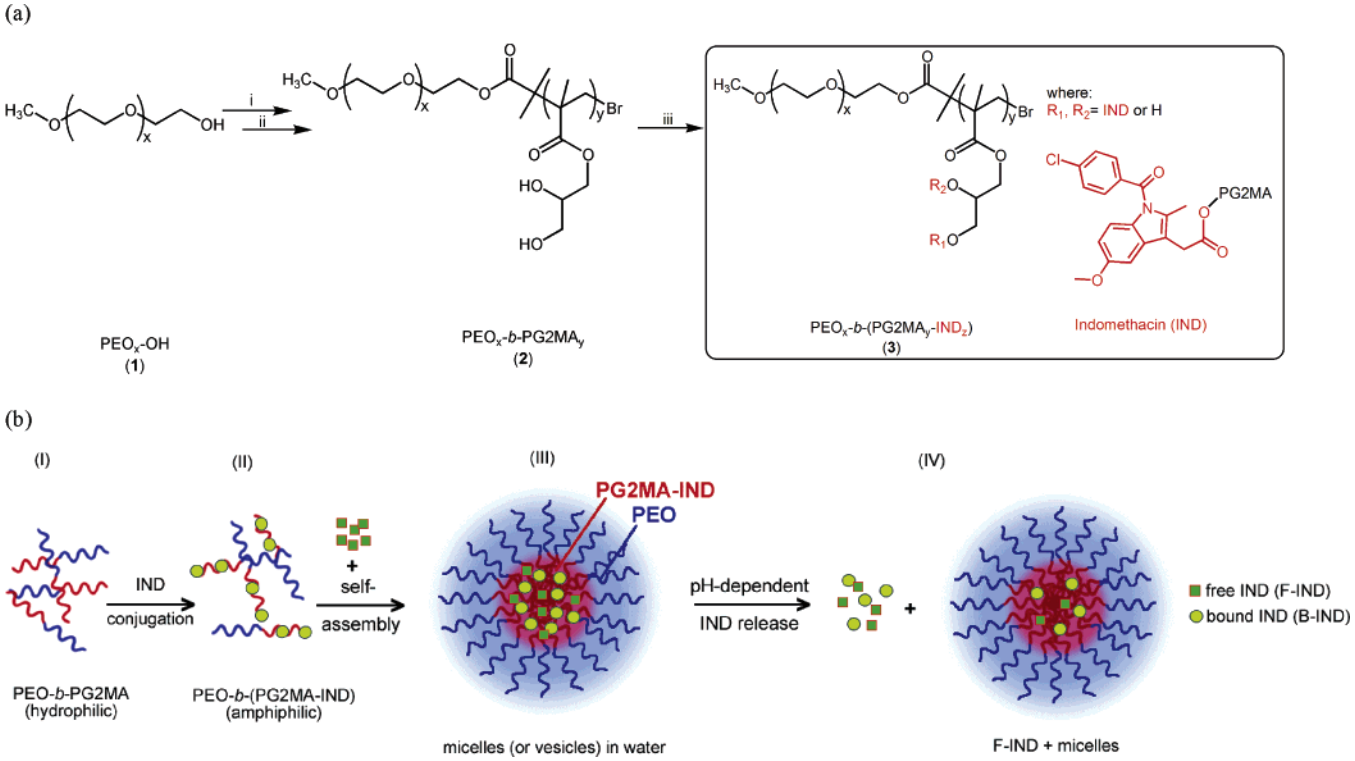

Figure 1. Synthesis (a) and solution behavior (b) of amphiphilic PEO-*b*-(PG2MA-IND) polymer−drug conjugates and their precursors: (i) α-bromoisobutyryl bromide, Et_3N, toluene, overnight, room temperature; (ii) G2MA, CuBr/bpy, MeOH, 20 °C; (iii) indomethacin, DCC/DMAP, DMF, 72 h, room temperature.

Table 1. ATRP of G2MA in MeOH at 20 °C Using CuBr/bpy as Catalyst, and Characteristics of Resulting PEO-*b*-PG2MA Diblock Copolymers

diblock PEO$_x$-*b*-PG2MA$_y$	time (h)	convn (%)	M_n (target)[a] (g/mol)	M_n (theo)[b] (g/mol)	M_n (NMR)[c] (g/mol)	M_w/M_n[d]
113−40	4.0	96	11 400	11 200	11 400	1.10
113−65	2.0	62	19 400	14 000	15 500	1.12
113−85	5.0	91	19 400	18 200	18 600	1.16

[a] At quantitative monomer conversion. [b] Calculated based on the conversion estimated by ^{1}H NMR in MeOD. [c] Determined by ^{1}H NMR measurements in D_2O using the initiator methoxy moiety as reference (Supporting Information, Figure S3). [d] Determined by GPC measurements in 1.0 g/L LiBr DMF at 60 °C with PS standards.

Table 2. Molecular Characteristics of PEO-*b*-(PG2MA-IND) Conjugates and Their Self-assembled Structures

entry	conjugate PEO$_x$-*b*-(PG2MA$_y$-IND$_z$)	targeted esterification degree (%)	achieved esterification degree (%)[a]	convn[a] (%)	no. of IND molecules per chain[a,b]	wt % B-IND[b]	$\phi_{PG2MA-IND}$[c]	$2R_H$[d] (nm)	μ_2/Γ^2 [e]	morphology [f]
1	113-(40−10)	25	18	72	14/10	21	0.33	24	0.10	M
2	113-(40−17)	50	25	50	20/17	33	0.49	36	0.12	M
3	113-(40−21)	50	28	56	22/21	40	0.56	64	0.08	M
4	113-(40−29)	100	52	52	42/29	49	0.68	ND[g]	ND[g]	ND[g]
5	113-(65−08)	25	08	32	11/08	15	0.22	24		M
6	113-(65−28)	50	25	50	33/28	39	0.56	80	0.15	V
7	113-(85−10)	25	06	24	11/10	16	0.22	ND[g]	ND[g]	ND[g]
8	113-(85−29)	50	24	48	40/29	32	0.50	100	0.17	V

[a] Calculated by ^{1}H NMR in DMF-d_7 on the basis of the integral ratio between aromatic IND proton at 6.9 ppm and methacrylate signal of PG2MA block between 1.6 − 0.5 ppm, after purification. [b] Determined by UV−vis spectroscopy using typical absorption maximum of IND (λ_{max}) at 320 nm. [c] Volume fraction of PG2MA-IND in the resulting polymer − drug conjugate, assuming that the polymer density is equal to 1.0 g/mL. [d] Hydrodynamic size of self-assembled PEO-*b*-(PG2MA-IND) particles, as assessed by DLS. [e] Polydispersity estimated by cumulants analysis of $C(q,t)$ autocorrelation functions recorded at 90° scattering angle. [f] Dominant morphology of self-assemblies in solution (M = micelles; V = vesicles). [g] Not determined. Either the polymer was not fully soluble in THF (entry 7) or partially precipitated during micellization (entry 4).

for $0.30 < \phi_{hydrophobic} < 0.70$, whereas vesicles are expected for $\phi_{hydrophobic} > 0.70$.[33,34] Therefore, self-assembly into spherical micelles is anticipated for most of the samples listed in Table 2 (see below), fulfilling the objective of preparing micelles with IND-based cores.

Self-Assembly Behavior of Block Copolymer— Drug Conjugates. The solution behavior of PEO-*b*-PG2MA and PEO-*b*-(PG2MA-IND) copolymers is schematized in Figure 1b, which is based on DLS measurements carried out for solutions corresponding to steps I−IV, as depicted in Figure 2. For instance, PEO_{113}-*b*-$PG2MA_{85}$ is a double hydrophilic diblock copolymer and dissolves molecularly in water (unimers with hydrodynamic size $2R_H$ = 6−8 nm, Figure 2a). However, it becomes amphiphilic upon conjugation to indomethacin, and the PEO_{113}-*b*-($PG2MA_{85}$-IND_{29}) polymer−drug conjugate can then be molecularly dissolved, for example, in THF (unimers with $2R_H$ = 7 − 10 nm in THF, Figure 2b). In these two later cases, very low scattered light intensities were recorded. The

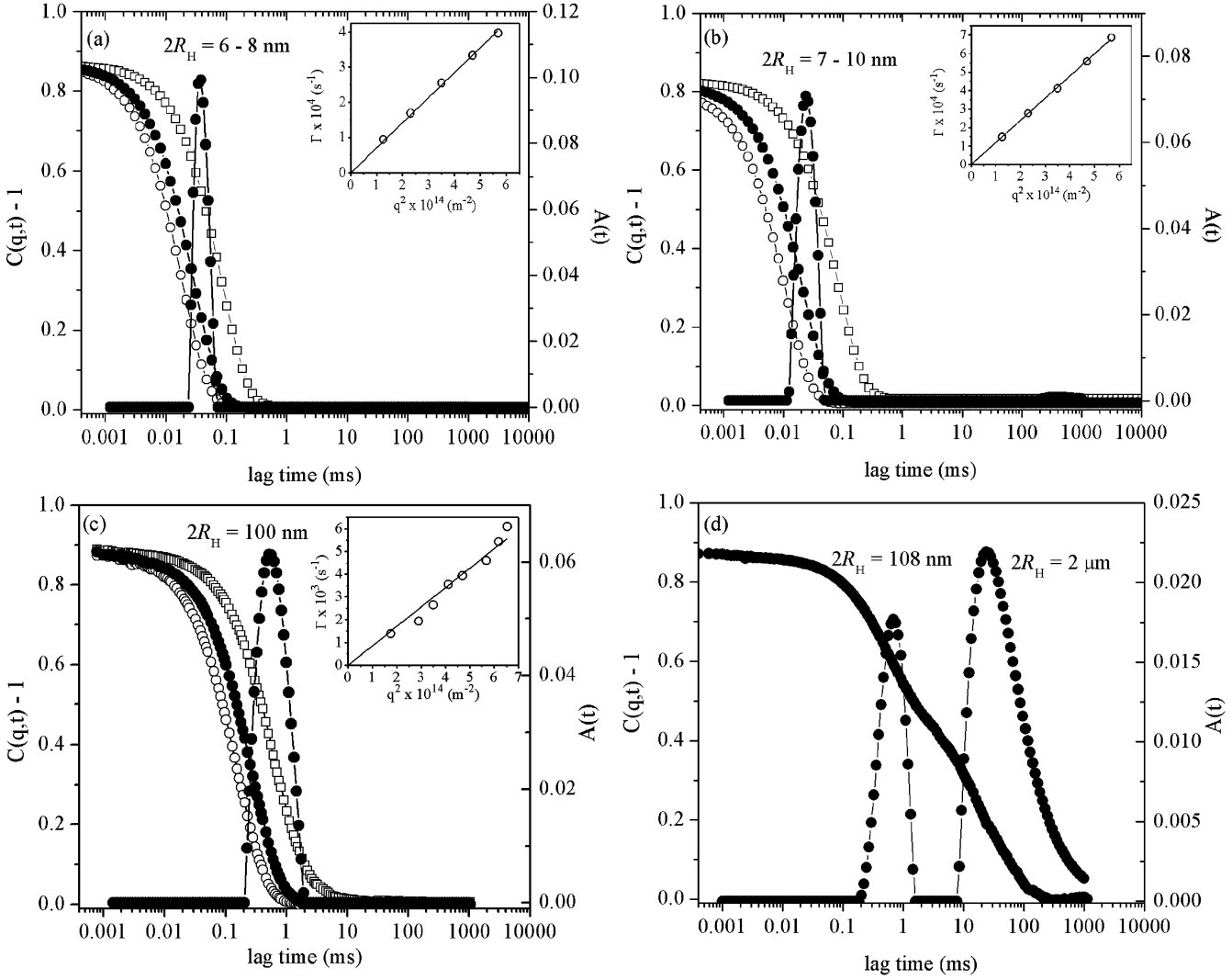

Figure 2. Autocorrelation functions $C(q,t)$ measured at scattering angles of 50 (□), 90 (●), and 130° (○), and distributions of the relaxation times $A(t)$ at 90° as revealed by CONTIN analysis for solutions corresponding to steps I−IV in Figure 1b, as follows: 10.0 mg/mL PEO_{113}-*b*-$PG2MA_{85}$ in water (a), 10.0 mg/mL PEO_{113}-*b*-($PG2MA_{85}$-IND_{29}) in THF (b), 0.5 mg/mL PEO_{113}-*b*-($PG2MA_{85}$-IND_{29}) in water (c), and 0.5 mg/mL PEO_{113}-*b*-($PG2MA_{85}$-IND_{29}) after 5 h in water at pH = 2.0−3.5 (d).

addition of a selective solvent (water at pH = 7.4) to situation II (Figure 1b) induces self-assembly, leading to well-defined spherical micelles (Figure 2c), which contain a hydrophobic drug linked covalently to the core through acid-sensitive ester bounds. The relaxation frequency is q^2-dependent (see insets) for all the systems, thus characterizing the diffusive behavior of scattering particles.

The nanoparticles structure and size was found to be dictated by both the length of PG2MA block and the amount of indomethacin (see below). The ability of these micelles to release active molecules in response to pH changes is illustrated in Figure 2d, which shows the autocorrelation function and distribution of relaxation times for the same solution as in Figure 2c, but after 5 h in an acidic environment (pH adjusted to 2.0−3.5). Under these circumstances, a very slow relaxation time appeared ($2R_H > 2$ μm), which was related to very large particles in solution formed by precipitation of free indomethacin within the sample holding cell, thus corroborating its pH-dependent release.

Figure 3 shows typical autocorrelation functions $C(q,t)$ measured at different scattering angles and distributions of the relaxation times $A(t)$ at 90° as revealed by CONTIN analysis for 1.0 mg/mL PEO-*b*-(PG2MA-IND) block copolymer−drug solutions in water. The insets in Figure 3 depict the typical q^2 dependence of the relaxation frequency (Γ) for diffusive scattering particles.[28] Thus, the $2R_H$ values discussed hereafter were calculated from the Stokes−Einstein relation (eq 5). In general, reasonably narrow distributions of relaxation times were obtained (μ_2/Γ^2 = 0.08−0.17, Table 2), with a fast dominant mode corresponding to the diffusive motion of individual particles (micelles or vesicles). For PEO_{113}-*b*-($PG2MA_{65}$-IND_{08}) solutions (Figure 3c) a slow mode associated with the existence of large aggregates (or other morphologies) was observed. However, the 6-fold difference in the relaxation frequency (and ultimately in the particles size) between the fast and slow modes should be considered to interpret these results. Even though the amplitude is higher for the slow mode than for the fast one, the number of particles with small size prevails because the light scattered intensity strongly depends on particle mass and size, implying that DLS reports an intensity-average size. Moreover, it is important to note that the amplitude of the two relaxation modes (slow and fast) strongly depends on the scattering angle in DLS measurements.[28]

The size and morphology of nano-objects originated from the self-assembly of PEO-*b*-(PG2MA-IND) block copolymer−drug solutions depended on both the amount of IND and the

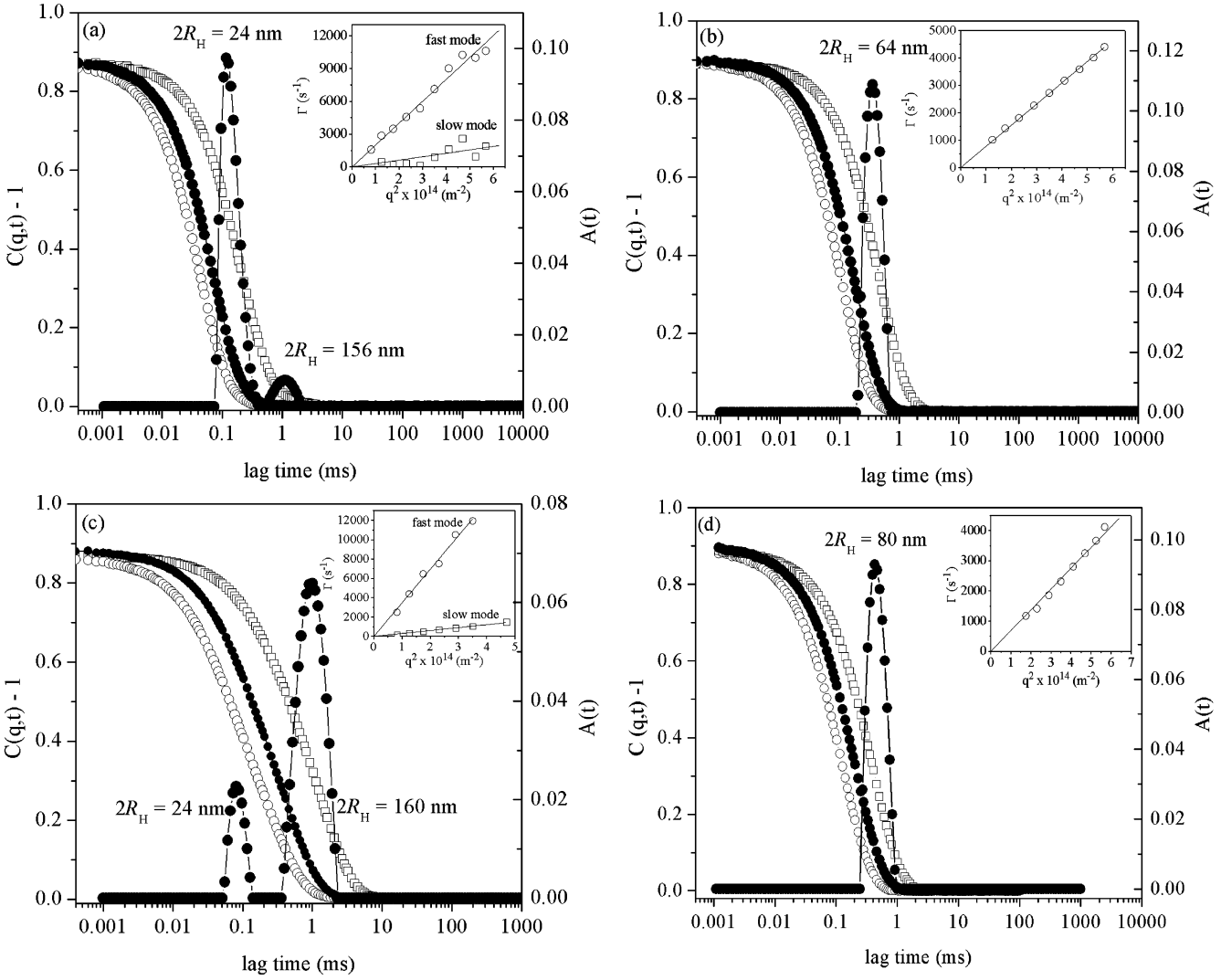

Figure 3. Autocorrelation functions $C(q,t)$ at scattering angles of 50 (□), 90 (●), and 130° (○), and distributions of the relaxation times $A(t)$ at 90° as revealed by CONTIN analysis for 1.0 mg/mL PEO_x-*b*-($PG2MA_y$-IND_z) block copolymer−drug solutions in water: 113-(40−10) (a), 113-(40−21) (b), 113-(65−08) (c), and 113-(65−28) (d).

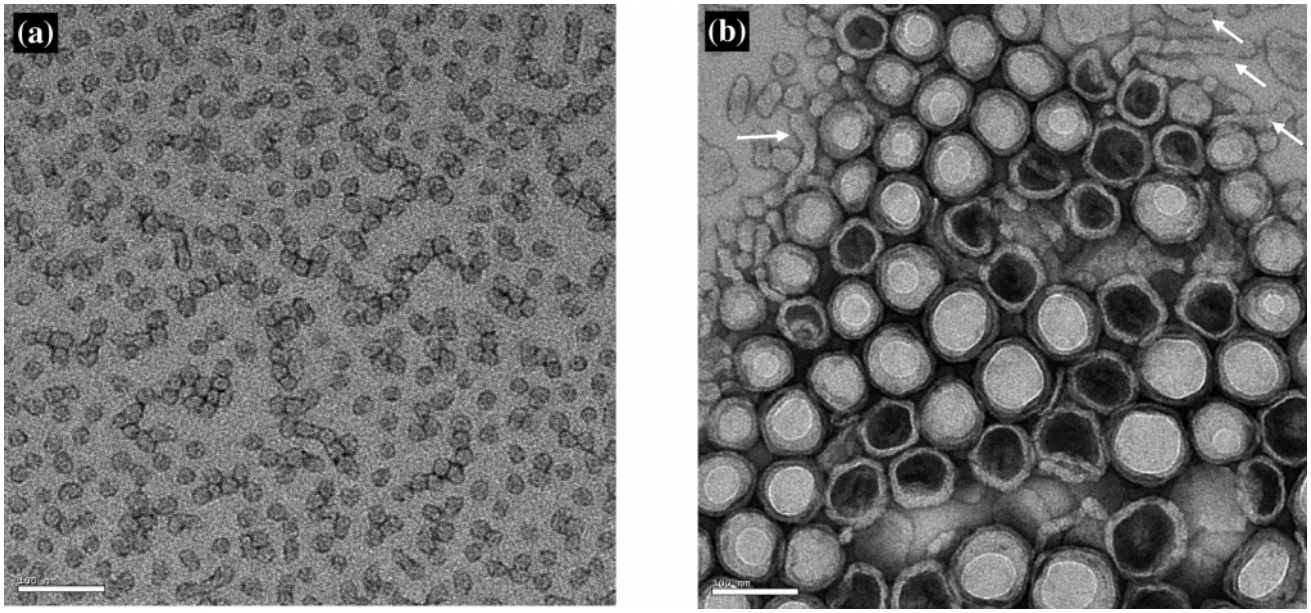

Figure 4. TEM images of unloaded PEO_x-*b*-($PG2MA_x$-IND_z) assemblies: 113-(40−10) (a) and 113-(65−28) (b). Scale bar is 100 nm.

PG2MA block length. For the shortest polymer precursor (PEO_{113}-*b*-$PG2MA_{40}$), spherical micelles with diameter ($2R_H$) varying from 24 to 64 nm were obtained with increasing IND contents (21−40 wt %) (Table 2, entries 1−3). According to

Table 3. Loading Results for IND Encapsulation by Nanoparticles Made from PEO-*b*-(PG2MA-IND) Conjugates

entry	conjugate PEO_x-*b*-($PG2MA_y$-IND_z)	C_p (mg/mL)	added F-IND (mg/mL)	L.E.[a] (%)	F-IND[b] (% w/wp)	B-IND (% w/wp)	total IND payload[c] (% w/wp)
1	113-(40−10)	1.0	0.5	40	20	21	41
2	113-(40−21)	1.0	0.5	36	18	40	58
3	113-(65−08)	1.0	0.5	27	13	15	28
4	113-(65−28)	1.0	0.5	44	15	39	54

[a] Loading efficiency calculated by eq 1. [b] Free IND content encapsulated inside the nanoparticles, as determined by UV−vis spectroscopy. [c] F-IND + B-IND.

static light scattering (SLS) measurements (Supporting Information, section 4), such a behavior is, besides the volume occupied by the drug, in part due to an increase in the respective aggregation number (N_{agg}) of the micelles in a process favored by hydrophobic interactions. These results are in very good agreement with other reports, which suggest that the length and the hydrophobic character of the core-forming block determine the micelle dimensions,[35,36] and consequently the loading efficiency, drug release profile, partition coefficient, bioavailability, and biodistribution of the carrier system.[36] The morphology of these nanoparticles was confirmed by TEM experiments, which are shown in Figure 4 for selected samples. In general, narrowly distributed nanosized spherical micelles were clearly identified as depicted in Figure 4, panel a, for PEO_{113}-*b*-($PG2MA_{40}$-IND_z) samples.

Very surprisingly, however, was the occurrence of kinetically stable vesicular structures with an average wall thickness of 12 nm by TEM for sample PEO_{113}-*b*-($PG2MA_{65}$-IND_{28}) (Figure 4, panel b), which presents $\phi_{G2MA-IND} = 0.56$. Normally, the formation of micelles is expected at this volume fraction of the hydrophobic segment.[33,34] The origin of such an observation surely relies on the polymer−drug conjugate structure. It can be noted that in spite of the hydrophobic character of this sample due to the presence of linked IND, it contains a number unsubstituted OH groups in the PG2MA block, thus generating an additional, and very important constraint during the micellization that might favor a transition from spheres to vesicles. During such a transition, an intermediate elongated or cylindrical morphology is usually observed for block copolymers systems either in organic or aqueous media.[34,37] In the present case, a few cylinders can indeed be identified in Figure 4, panel b, as indicated.

The mean nanoparticles (micelles and vesicles) diameter observed in TEM micrographs (for instance, $2R \sim 15-20$ nm for PEO_{113}-*b*-($PG2MA_{40}$-IND_{10}) (Figure 4a) and $2R \sim 60-70$ nm for PEO_{113}-*b*-($PG2MA_{65}$-IND_{28}) (Figure 4b)) are slightly smaller than those determined by DLS measurements ($2R_H$ = 24 nm for PEO_{113}-*b*-($PG2MA_{40}$-IND_{10}) (Figure 3a) and $2R_H$ = 80 nm for PEO_{113}-*b*-($PG2MA_{65}$-IND_{28}) (Figure 3d)). This is in part due to micelle dehydration caused by solvent evaporation under the high vacuum conditions employed during TEM imaging. However, discrepancies are also expected because DLS reports an intensity-average diameter, whereas TEM reports a number-average diameter. Thus, for a given size distribution of finite polydispersity, TEM images will usually undersize relative to DLS data. Overall, the size of PEO-*b*-(PG2MA-IND) nanodelivery system ($2R_H < 100 - 200$ nm) is considered ideal for avoiding the body's defense mechanisms (the reticuloendothelial system (RES).[5]

Indomethacin (IND) Loading. The ability of PEO-*b*-(PG2MA-IND) micelles to physically encapsulate free IND (F-IND) was assessed in order to further improve their loading capacity (i.e., total drug payload), in which the compatibility between solubilizate and micelle core is in principle high. A relationship between B-IND and F-IND can thus be anticipated for these systems, being indeed confirmed by entries 1 and 3 in Table 3, which shows loading results for selected samples at constant polymer and added IND concentrations. In these cases, the increase in B-IND from 15 to 21% w/w_p is accompanied by a parallel increase in F-IND from 13 to 20% w/w_p. As for other micellar drug carriers, the loading capacity is obviously finite, and a limitation of encapsulation F-IND there appears to exist as B-IND further increases (entries 2 and 4). The amounts of unbound or free IND (F-IND) effectively encapsulated by PEO-*b*-(PG2MA-IND) micelles as prepared in this work are comparable with those reported for other IND micellar delivery systems tested so far: 8−9% w/w_p for PEO-*b*-PLA;[19] 6−14% w/w_p for PEO-*b*-poly(alkyl (meth)acrylates);[18] 20% w/w_p for PEO-*b*-PBLA;[22] 17−42% w/w_p for PEO-*b*-PCL.[20,21]

Most importantly, however, is the remarkable total IND payload (i.e., covalently bound IND + physically entrapped IND) achieved using micellar nanocontainers formed by self-assembly of PEO-*b*-(PG2MA-IND) block copolymer−drug conjugates. IND contents ranging from 28 up to 58% w/w_p (Table 3) were systematically obtained by this facile approach, being entirely comparable with reports by Bertin et al.[23] (30−60% w/w_p) and Quémener et al.[24] (5−70% w/w_p).

Interestingly, it has been observed that self-organization for F-IND loaded samples with more than 50% w/w_p IND payload (Table 3, entries 2 and 4) either originated vesicular morphologies instead of micelles or provoked a huge increase in the size of vesicles. The distributions of the hydrodynamic diameter ($2R_H$) determined by DLS for unloaded and F-IND loaded PEO_x-*b*-($PG2MA_x$-IND_z) nanoparticles revealed a remarkable (~3-fold) increase in their size (for example, from $2R_H$ = 64 nm to $2R_H$ = 160 nm for PEO_{113}-*b*-($PG2MA_{40}$-IND_{21}) and from $2R_H$ = 80 nm to $2R_H$ = 220 nm for PEO_{113}-*b*-($PG2MA_{65}$-IND_{28})) with a parallel augmentation in the normalized scattered light intensity at a 90° scattering angle ($I_{sc}^{90}N$) (see insets) upon F-IND loading, as illustrated in Figure 5. These observations are in good agreement with results by TEM, which are shown in Figure 6 for the same systems as in Figure 5. Indeed, micrographs taken for F-IND loaded (Figure 6, panels a and b) and unloaded (Figure 6, insets in panels a and b) PEO-*b*-(PG2MA-IND) nanoparticles confirmed the existence of a morphology transition from spheres to vesicles (panel a) and/or an important size augmentation upon F-IND loading (panels a and b). Besides, slightly bluish aspects (visual inspection by digital photographs, not shown) were observed for such solutions, suggesting the presence of relatively large objects in solution. The wall thickness of 12 nm for vesicles formed by PEO_{113}-*b*-($PG2MA_{65}$-IND_{28}) diblocks practically did not change upon the addition of F-IND, as estimated from Figure 6, panel b, and the respective inset.

The results above suggest that the thermodynamics and kinetics of PEO-*b*-(PG2MA-IND) self-organization change dramatically in presence of F-IND, possibly leading to morphology transitions. This is an important observation as far as the structure and dynamics of block copolymer micellar drug delivery vehicles affect parameters such as hydrodynamic

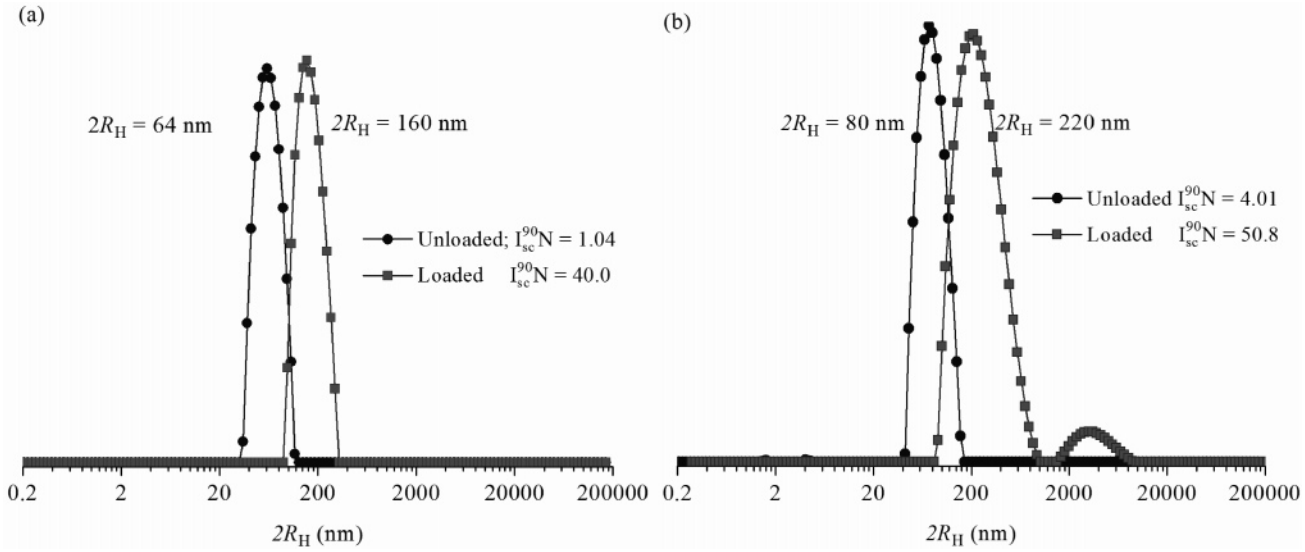

Figure 5. Distributions of the hydrodynamic diameter ($2R_H$) obtained by DLS using CONTIN analysis for F-IND loaded 1.0 mg/mL PEO_x-*b*-($PG2MA_x$-IND_z) block copolymer−drug nanoparticles in water: 113-(40−21) + 18% w/w_p F-IND (a) and 113-(65−28) + 15% w/w_p F-IND (b).

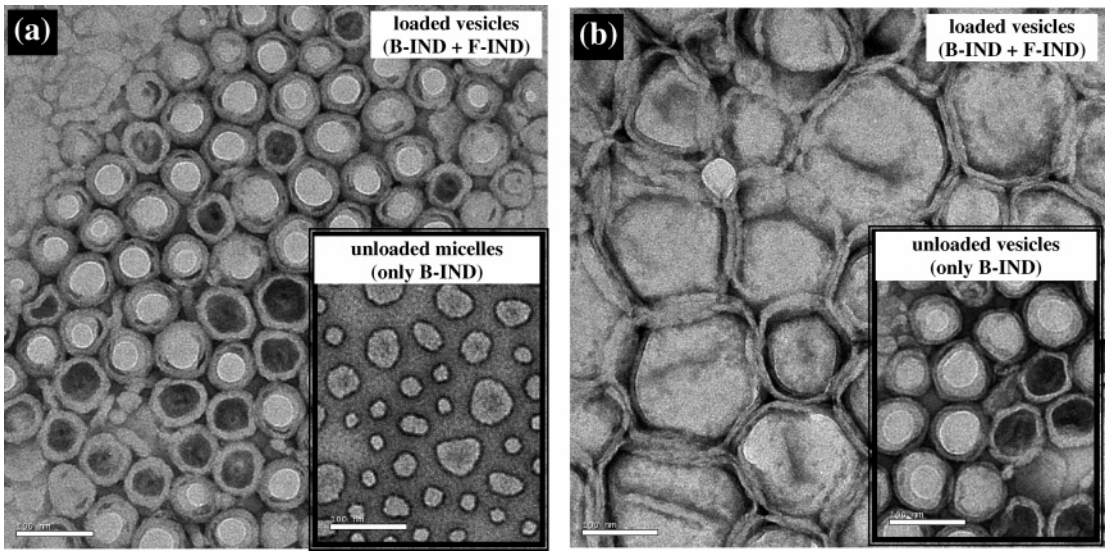

Figure 6. TEM images of F-IND loaded PEO_x-*b*-($PG2MA_x$-IND_z) assemblies: 113-(40−21) + 18% w/w_p F-IND (a) and 113-(65−28) + 15% w/w_p F-IND (b). Scale bar is 100 nm in all images, including the insets.

diameter, molar mass, etc., therefore exerting huge implications on nanoparticle biodistribution, drug loading capacity and release kinetics.[9]

In Vitro Release Kinetics. The release of drugs from block copolymer nanocarriers depends upon several physical-chemical parameters such as drug diffusion rate, partition coefficient between drug and hydrophobic segment, micelle/vesicle stability, and the copolymer biodegradation rate, among others. In the case of stimuli-responsive systems, these parameters can change dramatically as a function of the environmental surroundings, leading to triggered release processes.

Indomethacin release from PEO-*b*-(PG2MA-IND) micelles has been anticipated as being a pH-dependent phenomenon first due to intrinsic molecular characteristics of F-IND, and second due to pH-sensitivity of ester linkages in the conjugate. Physically encapsulated F-IND has a carboxylic acid group whose pK_a is 4.5.[22,38] As a result of its aqueous dissociation behavior, neutral (F-IND), and negatively charged ($F\text{-}IND^-$) species coexist in solution, and the respective molar fraction depends on the solution pH (Supporting Information, section 5). The overall aqueous solubility constant (K_s) of F-IND is, for this reason, strictly determined by its degree of protonation. The solubility of F-IND in pH 1.2 and pH 7.2 buffered aqueous media was found to be 0.011 and 2.1 mmol/L, respectively.[38] Therefore, F-IND can be considered as a practically insoluble drug at pH 1.2 and slightly soluble at pH 7.2 buffer solutions. The obvious difference in terms of K_s between F-IND and $F\text{-}IND^-$ species has been claimed by Kataoka et al.[22] to explain the higher release rate (>15-fold) of F-IND from micellar nanocarriers at neutral pH as compared to acidic media.

From a drug delivery standpoint, esters, carbonates, amides, and urethanes are linkers susceptible toward hydrolysis in acidic media, yielding to the so-called passive hydrolysis, and the rate of hydrolysis decreases in the order ester > carbonate > amides > uretanes.[39] Nevertheless, cleavage may also occur between the spacer and the polymeric backbone leading to the release of the spacer−drug moiety. The pH-dependent release of IND molecules linked to polymer chains via amide and anhydride bounds has been formerly reported elsewhere.[23,24]

In the present work, the release of IND from nanocarries originated from self-assembly of PEO-*b*-(PG2MA-IND) block copolymer−drug conjugates was investigated as a function of

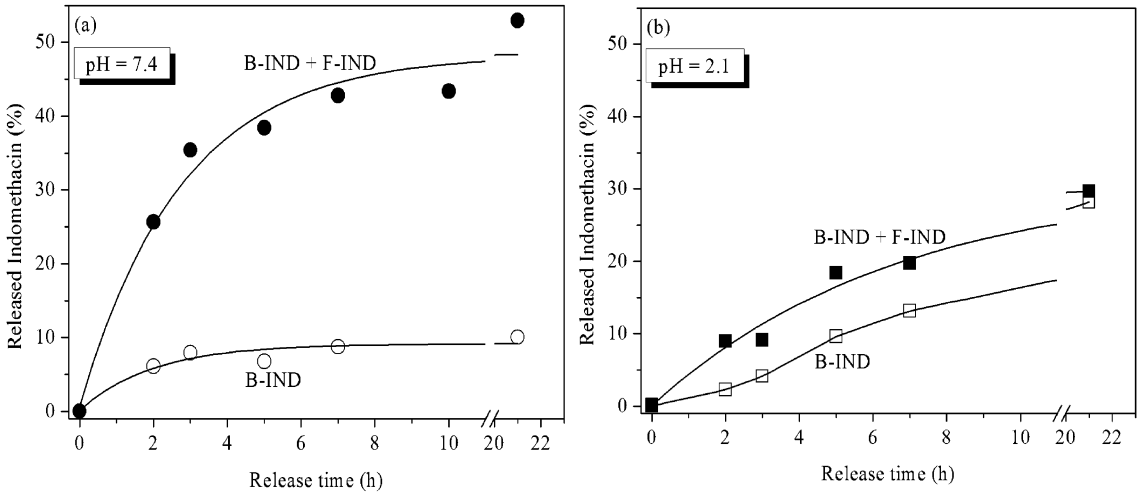

Figure 7. Percentage of IND released as a function of time as determined by variations in the UV absorbance at $\lambda_{max} = 320$ nm for 1.0 mg/mL PEO_{113}-*b*-($PG2MA_{40}$-IND_{21}) conjugates at pH = 7.4 (a) and pH = 2.1 (b) in absence and in presence of 0.18 mg/mL F-IND, as indicated.

the solution pH in absence and in presence of F-IND. Figure 7 shows the percentage of IND released over time as determined by variations in the UV absorbance at 320 nm (Figure S7). At pH = 7.4 and in the absence of F-IND (Figure 7a, open symbols), the amount of IND released from the nanoparticles increased slightly as a function of time. After a rapid release of ca. 10% of the initial IND payload (0.40 mg/mL) during the initial 2−3 h period, a quite stable plateau was systematically observed, suggesting that ester bound cleavage hardly occurred. This profile was interpreted as corresponding to the passive diffusion of a given amount (typically 10−20%) of unbound IND that could not be completely separated during purification by selective precipitation of block copolymer drug conjugates. Essentially the same comments also apply for other samples listed in Table 3. On the other hand, nanoparticles carrying both B-IND and F-IND (Figure 7a, filled symbols) produced 5-fold faster and sustained release rate (as illustrated in Higuchi plots, Figure S8) of their encapsulated content following an initial 2-h burst release. After 21 h, nearly 50% of the total IND payload (0.58 mg/mL) had been released. The undesirable burst effect normally takes place when a significant amount of the drug resides at the core−corona interface or in the corona, because molecules do not have to traverse large core segments to exit the carrier.[6]

Upon exposure to pH = 2.1 solutions, PEO-*b*-(PG2MA-IND) micellar solutions without added F-IND (Figures 7b, open symbols) exhibited sustained release with slow kinetics. Albeit it seems clear that acid medium favored acid hydrolysis of ester bounds, only 25% of total IND payload (0.40 mg/mL) diffused out of the nanoparticles during 21 h. Indeed, from this amount 15% consisted in hydrolyzed B-IND while ∼10% is F-IND (Figure 7a). Likewise, much slower release rate was observed in presence of F-IND (Figure 7b, filled symbols) (30% of 0.58 mg/mL released after 21 h). Interestingly, minor burst effect occurred at low pH in both cases. The pH-dependent release rate of F-IND herein characterized is in good agreement with previous reports by other research groups,[22,40] and can be attributed to the very different solubility of IND as a function of the solution pH, as mentioned above.

The passive hydrolysis of ester linkage in PEO-*b*-(PG2MA-IND) conjugates was found to be a rather slow process (15% release after 21 h exposure to pH = 2.1 solutions at room temperature), being fairly comparable with findings obtained by Bertin et al.[23] These authors determined that 20% of the amide-bound IND was released from the block copolymer-based nanoparticles after 48-h incubation at pH = 3.0 and at 37 °C. Nevertheless, our release studies indicated slower kinetics as compared to the hydrolysis of anhydride-bound IND in polynorbornene colloidal particles (80% release after 48-h incubation at pH = 3.0), as reported by Quémener et al.[24]

The release profiles observed for IND release from PEO-*b*-(PG2MA-IND) micellar nanoparticles emphasizes their excellent potential as drug delivery vehicles, as judged from their distinguished capacity to transport, retain and deliver indomethacin.

4. Conclusions

Well-defined double hydrophilic PEO-*b*-PG2MA copolymers ($M_w/M_n < 1.20$) synthesized by ATRP of G2MA in methanol using PEO macroinitiators can be used for post-polymerization conjugation to the hydrophobic nonsteroidal anti-inflammatory agent indomethacin (IND). The pendent hydroxyl groups of PG2MA segment, and carboxylic acid moiety of IND react under Steglich conditions to produce amphiphilic block copolymer−drug conjugates. Albeit quantitative conversions are not easily achievable, distinct drug contents can be covalently attached to the same polymer precursor, yielding macromolecules in which the IND content and volume fraction of G2MA-IND ($\phi_{G2MA-IND}$) range from 15 to 49 wt %, and from 0.22 to 0.68, respectively. The resulting amphiphilic PEO-*b*-(PG2MA-IND) conjugates self-assemble into nanometer-sized spherical micelles or vesicles in water, whose hydrodynamic size ($2R_H$) is dictated by both the amount of IND and the PG2MA block length. For all the samples investigated, the size for such a nanodelivery system ($2R_H \leq 100$ nm) was adequate for avoiding the body's defense mechanisms. The ability of these PEO-*b*-(PG2MA-IND) micelles to solubilize, transport and deliver IND can be further improved by physically encapsulating 13−20% w/w_p F-IND, thus reaching remarkable IND payloads (i.e., covalently bound IND + physically entrapped IND) ranging from 28 to 58% w/w_p. However, self-organization for F-IND loaded samples with more than 50% w/w_p IND payload favor the formation of stable vesicular morphologies instead of micelles and induce a significant increase in the size of the objects, as was highlighted by light scattering and imaging experiments. The IND release from PEO-*b*-(PG2MA-IND) micelles is a pH-dependent process. At approximately neutral pH the ester bound linkages are stable, and the diffusion of unbound and negatively charged $F\text{-}IND^-$ (deprotonated species) out of the carrier is favored due its obviously higher water

solubility. On the contrary, sustained release with slow kinetics normally takes place at acidic pH conditions, in which neutral F-IND species are much less soluble in the release medium, meanwhile passive acid hydrolysis of ester linkages takes place, thus allowing the release of B-IND.

Acknowledgment. R.B. acknowledges financial support from the CNRS, Université Bordeaux 1, Région Aquitaine, and FEDER. C.G. and V.S. thank, respectively, CAPES and the CNPq for the fellowships. The authors are grateful to Dr. A. R. Brisson for helpful discussions on the electron microscopy images and to Dr. J. Lai-Kee-Him and N. Guidolin for their technical assistance.

Supporting Information Available: Text giving experimental details, NMR and UV−vis analyses of diblock copolymers and their self-assembled structures, a table of physicochemical parameters, and figures showing a diagram of the experimental setup, GPC traces, ^{1}H NMR and UV-vis spectra, a diagram of species distribution, and a plot of diffusional release. This material is available free of charge via the Internet at http://pubs.acs.org.

References and Notes

(1) Matyjaszewski, K.; Davis, T. P. *Handbook of Radical Polymerization.* Wiley-Interscience: New York, 2002.
(2) Lodge, T. P.; Pudil, B.; Hanley, K. J. *Macromolecules* **2002**, *35*, 4707−4717.
(3) Discher, B. M.; Won, Y.-Y.; Ege, D. S.; Lee, J. C.-M.; Bates, F. S.; Discher, D. E.; Hammer, D. A. *Science* **1999**, *284*, 1143−1146.
(4) Riess, G. *Prog. Polym. Sci.* **2003**, *28*, 1107−1170.
(5) Allen, C.; Maysinger, D.; Eisenberg, A. *Colloids Surf. B: Biointerfaces* **1999**, *16* (1−4), 3−27.
(6) Soo, P. L.; Luo, L. B.; Maysinger, D.; Eisenberg, A. *Langmuir* **2002**, *18*, 9996−10004.
(7) Nishiyama, N.; Bae, Y.; Miyata, K.; Fukushima, S.; Kataoka, K. *Drug Discovery Today* **2005**, *2* (1), 21−26.
(8) Duncan, R. *Nat. Rev. Drug Discov.* **2003**, *2*, 347−360.
(9) Kwon, G. S.; Okano, T. *Adv. Drug Deliv. Rev.* **1996**, *21* (2), 107−116.
(10) Kataoka, K.; Harada, A.; Nagasaki, Y. *Adv. Drug Deliv. Rev.* **2001**, *47* (1), 113−131.
(11) Lu, Y.; Low, P. S. *Adv. Drug Deliv. Rev.* **2002**, *54*, 675−693.
(12) Bae, Y.; Jang, W. D.; Nishiyama, N.; Fukushima, S.; Kataoka, K. *Mol. Biosyst.* **2005**, *1*, 242−250.
(13) Licciardi, M.; Giammona, G.; Du, J. Z.; Armes, S. P.; Tang, Y. Q.; Lewis, A. L. *Polymer* **2006**, *47*, 2946−2955.
(14) Schmidt, V.; Giacomelli, C.; Lecolley, F.; Lai-Kee-Him, J.; Brisson, A. R.; Borsali, R. *J. Am. Chem. Soc.* **2006**, *128*, 9010−9011.
(15) Rodríguez-Hernández, J.; Chécot, F.; Gnanou, Y.; Lecommandoux, S. *Prog. Polym. Sci.* **2005**, *30*, 691−724.
(16) Ishihara, K.; Ueda, T.; Nakabayashi, N. *Polym. J.* **1990**, *22*, 355−360.
(17) Insel, P. A. Analgesic-antipyretics and antiinflammatory agents: drugs employed in the treatment of rheumatoid arthritis and gout. In *The Pharmacological Basis of Therapeutics*; Gilman, A. G., Rall, T. W., Nies, A. S., Taylor, P., Eds.; Pergamon Press: New York, 1990; pp 638−681.
(18) Sant, V. P.; Smith, D.; Leroux, J. C. *J. Controlled Release* **2004**, *97*, 301−312.
(19) Choi, S. K.; Kim, D. *J. Appl. Polym. Sci.* **2002**, *83*, 435−445.
(20) Shin, I. L. G.; Kim, S. Y.; Lee, Y. M.; Cho, C. S.; Sung, Y. K. *J. Controlled Release* **1998**, *51* (1), 1−11.
(21) Kim, S. Y.; Shin, I. L. G.; Lee, Y. M.; Cho, C. S.; Sung, Y. K. *J. Controlled Release* **1998**, *51* (1), 13−22.
(22) La, S. B.; Okano, T.; Kataoka, K. *J. Pharm. Sci.* **1996**, *85* (1), 85−90.
(23) Bertin, P. A.; Watson, K. J.; Nguyen, S. T. *Macromolecules* **2004**, *37*, 8364−8372.
(24) Quémener, D.; Héroguez, V.; Gnanou, Y. *J. Polym. Sci., Part A* **2005**, *43*, 217−229.
(25) Liu, S.; Weaver, J. V. M.; Tang, Y.; Billingham, N. C.; Armes, S. P.; Tribe, K. *Macromolecules* **2002**, *35*, 6121−6131.
(26) Giacomelli, C.; LeMen, L.; Borsali, R.; Lai-Kee-Him, J.; Brisson, A.; Armes, S. P.; Lewis, A. L. *Biomacromolecules* **2006**, *7*, 817−828.
(27) Provencher, S. W. *Makromol. Chem.* **1979**, *180*, 201−209.
(28) Brown, W. *Dynamic Light Scattering. The Method and Some Applications.* Oxford University Press Inc.: New York, 1993.
(29) Fujii, S.; Cai, Y.; Weaver, J. V. M.; Armes, S. P. *J. Am. Chem. Soc.* **2005**, *127*, 7304−7305.
(30) Bories-Azeau, X.; Merian, T.; Weaver, J. V. M.; Armes, S. P.; van den Haak, H. J. W. *Macromolecules* **2004**, *37*, 8903−8910.
(31) Sunder, A.; Bauer, T.; Mulhaupt, R.; Frey, H. *Macromolecules* **2000**, *33*, 1330−1337.
(32) Sunder, A.; Quincy, M.-F.; Mülhaupt, R.; Frey, H. *Angew. Chem., Int. Ed.* **1999**, *38*, 2928−2930.
(33) Bates, F. S.; Fredrickson, G. H. *Annu. Rev. Phys. Chem.* **1990**, *41*, 525−557.
(34) Discher, D. E.; Ahmed, F. *Annu. Rev. Biomed. Eng.* **2006**, *8*, 323−341.
(35) Mountrichas, G.; Mpiri, M.; Pispas, S. *Macromolecules* **2005**, *38*, 940−947.
(36) Soo, P. L.; Lovric, J.; Davidson, P.; Maysinger, D.; Eisenberg, A. *Mol. Pharm* **2005**, *2*, 519−527.
(37) Jain, S. J.; Bates, F. S. *Science* **2003**, *300*, 460−464.
(38) Nokhodchi, A.; Javadzadeh, Y.; Siahi-Shadbad, M. R.; Barzegar-Jalali, M. *J. Pharm. Pharm. Sci.* **2005**, *8* (1), 18−25.
(39) Soyez, H.; Schacht, E.; Vanderkerken, S. *Adv. Drug Deliv. Rev.* **1996**, *21* (2), 81−106.
(40) Albin, P.; Markus, A.; Pelah, Z.; Ben-Zvi, Z. *J. Controlled Release* **1994**, *29* (1−2), 25−39.

MA062562U